Microbiology (2007), **153**, 2491–2504 DOI 10.1099/mic.0.2006/005587-0

Transcriptional profiling of *Corynebacterium glutamicum* metabolism during organic acid production under oxygen deprivation conditions

Masayuki Inui, Masako Suda, Shohei Okino, Hiroshi Nonaka, László G. Puskás, Alain A. Vertès and Hideaki Yukawa

Research Institute of Innovative Technology for the Earth (RITE), 9-2 Kizugawadai, Kizugawa, Kyoto, 619-0292, Japan

Correspondence
Hideaki Yukawa
mmg-lab@rite.or.jp

Received 9 January 2007
Revised 4 March 2007
Accepted 10 April 2007

A transcriptional profiling of the metabolism of *Corynebacterium glutamicum* under oxygen deprivation conditions is reported. It was observed that the glucose consumption rate per cell when *C. glutamicum* cells were incubated under oxygen deprivation conditions was higher than that achieved by cells incubated under aerobic growth conditions. Furthermore, DNA microarray and quantitative RT-PCR analyses revealed that the genes of several key enzymes of the glycolytic and organic acid production pathways, including *gapA, pgk, tpi, ppc, ldhA* and *mdh*, were significantly upregulated under oxygen deprivation conditions. The corresponding enzymic activities consistently correlated with the regulation patterns of the genetic expression observed at the transcriptional level. Studies of *lacZ* fusions with the *gapA, ldhA* and *mdh* genes indicated not only that these genes are strongly induced at the onset of the stationary phase under aerobic growth conditions, but also that high expression levels are maintained under oxygen deprivation conditions. These results indicate that the genetic expression of several key metabolic enzymes in *C. glutamicum* cells incubated under oxygen deprivation conditions is chiefly regulated at the transcriptional level. The physiological consequence of the observed increased transcription under oxygen deprivation conditions is an increased rate of carbon source consumption, which is accompanied by a concomitant increase in organic acid production.

INTRODUCTION

Corynebacterium glutamicum is widely used as a cost-effective bioconverter for the industrial production of numerous metabolites, including amino acids and organic acids (Eggeling & Sahm, 1999; Hermann, 2003; Inui *et al.*, 1999a; Kelle *et al.*, 2005; Kumagai, 2000; Vertès *et al.*, 2005), as well as heterologous proteins (Billman-Jacobe *et al.*, 1995; Salim *et al.*, 1997). We previously observed that when aerobically grown *C. glutamicum* R (Yukawa *et al.*, 2007) is packed to a high cell density under oxygen deprivation conditions, despite the cessation of cellular growth, the cells remain able to excrete in significant amounts several metabolites, including lactate and succinate (Inui *et al.*, 2004b). There are two main advantages of using these oxygen deprivation conditions for the production of organic acids in corynebacteria. First, energy is primarily used for compound production, since microbial growth is essentially halted. This results in high yields and low by-product formation. Second, the absence of growth enables the use of micro-organisms at high density. This leads to high volumetric productivity.

The metabolism of *C. glutamicum* R for organic acid production has previously been investigated by measuring organic acid production, glucose consumption and intracellular NAD^+/NADH ratios in the wild-type and various mutant strains in which the genes coding for key metabolic enzymes have been inactivated (Inui *et al.*, 2004b). For L-lactate production, glucose is metabolized to pyruvate via

Abbreviations: DCW, dry cell weight; DO, dissolved oxygen; FUM, fumarase; GAPDH, glyceraldehyde-3-phosphate dehydrogenase; LDH, lactate dehydrogenase; MDH, malate dehydrogenase; MQO, malate: quinone oxidoreductase; OAA, oxaloacetate; ORP, oxidation–reduction potential; PC, pyruvate carboxylase; PEPC, phosphoenolpyruvate carboxylase; PGK, phosphoglycerate kinase; SDH, succinate dehydrogenase; TCA cycle, tricarboxylic acid cycle; TPI, triosephosphate isomerase.

The GenBank/EMBL/DDBJ accession nos for the complete *C. glutamicum* R genome DNA and native episome sequences are AP009044 and AP009045, respectively.

The array data discussed in this publication have been deposited in GenomeNet EXPRESSION (http://www.genome.jp/kegg/expression/) and are accessible through accession number ex0001754.

Tables showing oligonucleotides used in this study, expression data of genes observed to be up- or down-regulated under oxygen deprivation conditions, and the COGs functional annotation of genes and the numbers of genes showing increased or decreased transcriptional levels during oxygen deprived reactions, are available as supplementary data with the online version of this paper.

the glycolytic pathway. Pyruvate is in turn converted to L-lactate by the action of NAD-dependent lactate dehydrogenase (LDH). On the other hand, for succinate production, phosphoenolpyruvate, also metabolized from glucose, is converted to oxaloacetate (OAA) by the action of phosphoenolpyruvate carboxylase (PEPC), an anaplerotic enzyme. OAA is subsequently metabolized to succinate using the reductive arm of the tricarboxylic acid (TCA) cycle (i.e. OAA→malate→fumarate→succinate). The observation that under oxygen deprivation conditions PEPC is the predominant anaplerotic enzyme for succinate production (Inui *et al.*, 2004b) is particularly noteworthy, as under aerobic conditions it is pyruvate carboxylase (PC) which is known to be the predominant anaplerotic enzyme to replenish OAA pools for the production of amino acids such as glutamate or lysine (Peters-Wendisch *et al.*, 2001). In addition, the metabolism of *C. glutamicum* R under oxygen deprivation conditions is controlled mainly by the intracellular NAD^+/NADH ratio. Moreover, bicarbonate or pyruvate addition into the oxygen deprived reaction can act as a trigger to stimulate the glycolytic pathway. This phenomenon is known as the 'pump-priming effect' (Inui *et al.*, 2004b). Presumably, the uptake of extracellular pyruvate enables the regeneration of NAD^+ to fuel the glycolytic pathway at the glyceraldehyde-3-phosphate dehydrogenase (GAPDH) step.

To harness oxygen deprived metabolism in corynebacteria, we have developed a new, high-productivity bioprocess for organic acid production based on these observations (Inui *et al.*, 2004b; Okino *et al.*, 2005). Furthermore, we have recently applied this concept to the production of ethanol from recombinant *C. glutamicum* (Inui *et al.*, 2004a).

The present study aims at a better understanding of the physiological mechanisms underlying the performance of *C. glutamicum* for organic acid and ethanol production under process conditions of oxygen deprivation, as controlled at the level of the regulation of genetic expression. We used global DNA microarrays to establish complete transcription profiles of the *C. glutamicum* genome, in which cells were incubated under normal aeration conditions in A rich medium at physiological cell densities and under oxygen deprivation conditions in BT minimal medium at very high cell densities. These incubation conditions are referred to in the rest of this manuscript as 'aerobic conditions' and 'oxygen deprivation conditions', respectively.

METHODS

Bacterial strains and plasmids. The bacterial strains and plasmids used in this study are listed in Table 1.

Chemicals. All chemicals were of the highest available purity, and were purchased from Wako Pure Chemical Industries or Sigma.

Conditions for growth and organic acid production. For genetic manipulations, *Escherichia coli* strains were grown at 37 °C in Luria–Bertani (LB) medium (Sambrook *et al.*, 1989) and *C. glutamicum* strains were grown at 33 °C in A medium (2 g yeast extract l^{-1}, 7 g Casamino acids l^{-1}, 2 g urea l^{-1}, 7 g $(NH_4)_2SO_4$ l^{-1}, 0.5 g KH_2PO_4 l^{-1}, 0.5 g $K_2H_2PO_4$ l^{-1}, 0.5 g $MgSO_4 . 7H_2O$ l^{-1}, 6 mg $Fe_2SO_4 . 7H_2O$ l^{-1}, 4.2 mg $Mn_2SO_4 . H_2O$ l^{-1}, 0.2 mg biotin l^{-1}, 0.2 mg thiamine l^{-1}) with 4% glucose on a rotary shaker at 200 r.p.m. When appropriate, media were supplemented with antibiotics. The final antibiotic concentrations for *E. coli* were 50 μg tetracycline ml^{-1} and 50 μg chloramphenicol ml^{-1}; for *C. glutamicum,* the final antibiotic concentrations were 5 μg chloramphenicol ml^{-1} and 50 μg kanamycin ml^{-1}.

Corynebacteria were cultivated at 33 °C, pH 7.6, for 13 h in 500 ml A medium containing 4% glucose in a 1 l jar fermenter (BMJ01PI, Biott). The aeration was set at 1 l min^{-1} and the agitation speed was 1000 r.p.m. The culture was harvested by centrifugation at 6500 ***g*** and 4 °C for 15 min. The cell pellet was subsequently washed once with minimal medium (BT medium), which differs from the A medium by the absence of yeast extract and Casamino acids. For organic acid production under oxygen deprivation conditions, washed cells were resuspended at a final cell wet cell concentration of 50 g l^{-1} with 80 ml BT medium containing 200 mM glucose and 400 mM bicarbonate. The cell suspension was incubated at 33 °C with constant agitation without aeration in a lidded 100 ml medium bottle. The pH of the cell reaction was maintained at 8 using a pH controller (DT-1023, Biott) to supplement the medium with NH_3.

Analytical methods. Reaction mixtures were centrifuged (1000 ***g***, 4 °C, 1 min), and the supernatants were analysed for sugars and organic acids. Organic acids were quantified by HPLC (8020, Tosoh) equipped with an electric conductivity detector. The concentration of glucose was measured by an enzyme electrode glucose sensor (BF-4, Oji Scientific Instruments). Cell growth was monitored by measuring OD_{610} with a spectrophotometer (DU640, Beckman Coulter).

Detection methods for dissolved oxygen (DO) and oxidation–reduction potential (ORP). The concentration of DO and the ORP were continuously monitored using an oxygen electrode (Type 12, Biott) and a Redox Fermprobe (Broadley-James), respectively.

Enzymic assays. Cultures were harvested by centrifugation at 5000 ***g*** and 4 °C for 10 min. The cell pellet was washed once with extract buffer (100 mM Tris/HCl, pH 7.5, 20 mM KCl, 20 mM $MgCl_2$, 5 mM $MnSO_4$, 0.1 mM EDTA, 2 mM DTT). Cell suspensions were sonicated using an ultrasonic homogenizer (Astrason model XL2020) in an ice–water bath for three 2 min periods, interrupted by 2 min cooling intervals. Cell debris was removed by centrifugation (10 000 ***g***, 4 °C, 30min). The supernatant was used as a crude extract for enzyme assays. Protein concentrations were measured with a Bio-Rad protein assay kit.

Assays for GAPDH (Omumasaba *et al.*, 2004), phosphoglycerate kinase (PGK) (Eikmanns, 1992), triosephosphate isomerase (TPI) (Eikmanns, 1992), PEPC (Inui *et al.*, 1997) and LDH (Bunch *et al.*, 1997) were performed as previously described. Malate dehydrogenase (MDH) activity was determined as described by Sridhar *et al.* (2000), modified by using 0.1 M Tris/HCl (pH 8.0) and 0.15 mM NADH to obtain optimum enzyme activities. β-Galactosidase activities were measured as described previously (Inui *et al.*, 1999b).

DNA techniques. Plasmid DNA was isolated by the alkaline lysis procedure (Sambrook *et al.*, 1989) or by using a HiSpeed Plasmid Midi kit (Qiagen) according to the manufacturer's instructions, modified, when extracting DNA from corynebacteria, by using 4 mg lysozyme ml^{-1} at 37 °C for 30 min. Chromosomal DNA was isolated from corynebacteria following the method of Sambrook *et al.* (1989), modified by using 4 mg lysozyme ml^{-1} at 37 °C for 30 min. Restriction endonucleases and Klenow fragment were purchased from Takara and used as per the manufacturer's instructions. PCR was

Table 1. Bacterial strains and plasmids used in this study

Strain or plasmid	Relevant characteristics	Source or reference
Strains		
E. coli		
JM109	*recA1 endA1 gyrA96 thi hsdR17 supE44 relA1* Δ(*lac-proAB*)/F′[*traD36 proAB*$^+$ *lacI*^{q} *lacZ*ΔM15]	Takara
JM110	*dam dcm supE44 hsdR17 thi leu rpsL lacY galK galT ara tonA thr tsx* Δ(*lac-proAB*)/F′[*traD36 proAB*$^+$ *lacI*^{q} *lacZ*ΔM15]	Sambrook *et al.* (1989)
C. glutamicum		
R	Wild-type	Yukawa *et al.* (2007)
mdh mutant	*mdh*::Km^r	This work
sdhA mutant	*sdhA*::Km^r	This work
Plasmids		
pMC1871	Tc^r; *lacZ* fusion vector	Pharmacia
pHSG398	Cm^r; α *lac* multicloning site, M13 *ori*	Takara
pUC4K	Ap^r Km^r; source of Km^r cartridge	Pharmacia
pCRA725	Km^r; the suicide vector containing the *B. subtilis sacB* gene	Inui *et al.* (2004a)
pCRA740	Km^r; pCRA725 with a 2.0 kb PCR fragment from ISSs 7	This work
pCRA741	Km^r; pCRA740 with a 3.1 kb PCR fragment containing the *E. coli lacZ* gene	This work
pCRA742	Km^r; pCRA741 with a 0.6 kb PCR fragment containing the *C. glutamicum* R *gapA* promoter region	This work
pCRA743	Km^r; pCRA741 with a 0.4 kb PCR fragment containing the *C. glutamicum* R *ldhA* promoter region	This work
pCRA744	Km^r; pCRA741 with a 0.4 kb PCR fragment containing the *C. glutamicum* R *mdh* promoter region	This work
pCRA745	Cm^r; pHSG398 with a 1.0 kb *Bam*HI–*Sph*I fragment containing the *C. glutamicum* R *mdh* gene	This work
pCRA746	Cm^r Km^r; pCRA746 with a blunt-end-treated 1.2 kb fragment of Km^r cartridge inserted into the *Bgl*II site	This work
pCRA747	Cm^r; pHSG398 with a 2.0 kb *Sph*I fragment containing the *C. glutamicum* R *sdhA* gene	This work
pCRA748	Cm^r Km^r; pCRA748 with a blunt-end-treated 1.2 kb fragment of Km^r cartridge inserted into the *Stu*I site	This work

performed using an Applied Biosystems GeneAmp PCR System 9700 in a total volume of 100 µl with 50 ng chromosomal DNA, 0.5 µM each primer, 0.2 mM dNTP, 2 % DMSO in ExTaq polymerase buffer with $MgCl_2$ and 4 U ExTaq DNA polymerase (Takara) for 30 cycles at temperatures of 94 °C for denaturation (1 min), 55 °C for annealing (1 min), and 72 °C for extension (2 min). The PCR fragments were purified with a QIAquick PCR purification kit (Qiagen).

Corynebacteria were transformed by electroporation as previously described (Vertès *et al.*, 1993a). Transformation of *E. coli* cells was performed by the $CaCl_2$ procedure, as described by Sambrook *et al.* (1989).

Preparation of DNA microarray. PCR primers (20-mers) were designed to amplify the full-length coding DNA segments of 3080 predicted ORFs based on the annotation of the complete *C. glutamicum* R genome sequence (Yukawa *et al.*, 2007). Amino-terminus primers amplified 20 bp downstream from the initiation codon, which was included. Carboxy-terminus primers amplified 20 bp upstream from the termination codon, which also was included. The ORF-specific double-stranded DNA fragments were produced by standard PCR amplification methods, as described above, with genomic DNA of *C. glutamicum* R as template and the above primer sets. Each PCR product was analysed routinely by agarose gel electrophoresis to ensure its size and purity. When PCR products of the expected size or purity were not obtained, modification of PCR conditions, redesign of primer pairs, or purification of DNA fragments from gels were attempted. As a result, a library of 3076 single PCR products was obtained that contained 99.9 % of a total of 3080 predicted ORFs present in the *C. glutamicum* R genome. PCR products were purified by a PCR96 Cleanup kit (Millipore), desiccated and resuspended in Solution-T (Takara Bio). The PCR products thus obtained were printed in duplicate at two separate positions onto a 1 × 3 inch (2.5 × 7.5 cm approx.) Takara slide glass TX704 (Takara Bio) using an arraying robot. The DNA microarrays were rehydrated in a humidity chamber at 37 °C for 1 h. They were subsequently exposed to UV light at an energy setting of 60 mJ cm^{-2} in a UV cross-linker, and soaked in 0.2 % SDS for 2 min at room temperature. After being washed twice with ultrapure water, the slides were immersed in a succinic anhydride solution for 20 min at room temperature, and placed in boiling water for 2 min. The slides were then immersed in 100 % ethanol for 1 min and dried by centrifugation at 185 ***g*** for 2 min. Spotting quality was assessed by checking as controls the configuration and concentration of non-specific stained DNA spots on the DNA microarrays. In addition, 12 spots each of human transferrin receptor (1 kb), *E. coli* plasmid pUC19 and λDNA were printed onto the slides as negative controls

for DNA hybridization. DNA microarrays were stored at room temperature in the dark under controlled-humidity conditions until use.

RNA isolation. Total RNA was extracted from *C. glutamicum* R cells using the Qiagen RNeasy Midi kit. Cultures were added to two volumes of RNAprotect Bacteria reagent (Qiagen), incubated for 5 min, and centrifuged at 3000 r.p.m. for 5 min at room temperature. The pellet was resuspended in RLT buffer containing β-mercaptoethanol (RNeasy Midi kit, Qiagen) to a final concentration of 1 g dry cell weight (DCW) per litre. A 1 ml sample of this cell suspension was subsequently mixed with 0.5 g 0.1 mm zirconia/silica beads (BioSpec Products). Cells were mechanically disrupted for eight cycles of 45 s at a speed rating of 6.5 spaced by 5 min resting intervals in a FastPrep FP120 instrument (Qbiogene). The resulting mixture was centrifuged for 5 min at 15 000 r.p.m. The supernatant was processed using an RNeasy system (Qiagen) with DNase on-column treatment according to the manufacturer's instructions for RNA extraction. Isolated RNA samples were checked for purity by both agarose gel electrophoresis and spectrophotometric analysis, and stored at −80 °C until use.

Preparation of labelled cDNA. Fluorescently labelled cDNAs were prepared by cDNA synthesis with random nonamer primers and 30 μg total RNA of *C. glutamicum* R as template, with subsequent Cy3/Cy5 labelling, using a CyScribe cDNA Post-Labelling kit (Amersham Biosciences), according to the manufacturer's instructions.

Hybridization and analysis. Fifty microlitres of each Cy3- and Cy5-labelled cDNA probe, prepared as mentioned above, was mixed and added to 100 μl 2 × hybridization buffer [12 × saline sodium citrate (SSC), 0.4 % SDS, 10 × Denhardt's solution, 0.2 mg ml^{-1} denatured salmon sperm DNA]. All steps, from hybridizing to washing and drying, were automatically performed using a Lucidea Automated Slide Processor (Amersham Biosciences). The hybridization solution, which was heated at 95 °C for 2 min and cooled to room temperature, was added to hybridization buffer to a final combined volume of 200 μl. The DNA microarray was inserted into the Lucidea Automated Slide Processor and hybridization at 60 °C with the whole-genome DNA microarray was allowed to proceed for 14 h. The hybridization arrays were subsequently washed (once at 35 °C for 6 min in 2 × SSC and 0.2 % SDS, once at 35 °C for 6 min in 0.2 × SSC and 0.2 % SDS), rinsed (twice at 35 °C in 0.2 × SSC and once at 37 °C in isopropanol) and dried. The slides were scanned at 532 nm for Cy3 and at 635 nm for Cy5 with a Fujifilm Fluorescent Image Analyser FLA-8000 (Fuji). Images were analysed with a GenePix Pro 5.0 instrument (Axon Instruments). Individual spots were located, the Cy3 and Cy5 fluorescence intensity at each spot was measured, and the background signal intensities were determined. Artefacts on slides such as dust, scratches or salts were excluded from further analysis. Data analysis was performed using GeneSpring 6.1 software (Silicon Genetics). The data generated by GenePix 5.0 were loaded to GeneSpring 6.1 and normalized by global normalization and intensity-dependent LOWESS normalization to eliminate Cy dye bias. The normalization parameter selected in the GeneSpring 6.1 software was 'Per spot and per chip: intensity dependent (LOWESS) normalization'. The resultant raw intensity data were consecutively calculated as Cy3/Cy5 ratios that represented the average of a total of 12 hybridization signals for each gene: duplicate spots on six different slides of six replicate RNA samples from six independent biological samples. Negative controls consistently gave hybridization signals that were similar to the background. Estimated differences were considered significant if the P value of a t test was <0.05.

Quantitative RT-PCR. Quantitative RT-PCR was performed using an ABI PRISM 7000 Sequence Detection System (Applied Biosystems) and a QuantiTect SYBR Green RT-PCR kit (Qiagen) according to the manufacturer's instructions. Specific primers (primers 1–40 and 66–81) (Supplementary Table S1) were designed by the Primer Express Software version 2.0 (Applied Biosystems). Each PCR reaction consisted of 25 μl 2 × QuantiTect SYBR Green RT-PCR Master Mix, 0.5 μM forward primer, 0.5 μM reverse primer, 0.5 μl QuantiTect RT Mix and 50 ng total RNA in a total volume of 50 μl. PCR parameters were 50 °C for 30 min, 95 °C for 15 min, and 45 cycles at 95 °C for 15 s, 55 °C for 30 s, 72 °C for 30 s. The comparative C_T method (Applied Biosystems) was used to quantify relative expression, with a threshold cycle (C_T) being defined as the cycle at which the reporter fluorescence is distinguishable from the background in the extension phase of the PCR reaction. The C_T values were computed as the mean of triplicates.

Construction of *gapA–*, *ldhA–* and *mdh–lacZ* fusions. β-Galactosidase was expressed as hybrid *gapA′–*, *ldhA′–* and *mdh′–′lacZ* fusion proteins, using the native *gapA*, *ldhA* and *mdh* transcriptional and translational signals, respectively. In order to integrate the fusion genes on the *C. glutamicum* R chromosome by homologous recombination, a 2.0 kb DNA fragment from the strain-specific island 7 (SSI 7) (Suzuki *et al.*, 2005) of *C. glutamicum* R was amplified using the two oligonucleotide primers 41 and 42 with *C. glutamicum* R chromosomal DNA as template. The 2.0 kb PCR product was digested with *Sph*I, and inserted into the unique *Sph*I site of the suicide vector pCRA725, yielding pCRA740. The *E. coli lacZ* gene was amplified using oligonucleotide primers 43 and 44 with the *E. coli lacZ* fusion vector pMC1871 as template. The 3.1 kb PCR product containing the *E. coli lacZ* was digested with *Nhe*I, and inserted into the unique *Nhe*I site of pCRA740, yielding pCRA741. In order to amplify the *gapA* promoter region, the oligonucleotide primers 45 and 46 were used in a PCR with *C. glutamicum* R chromosomal DNA as template. The 0.6 kb PCR product encompassing the *gapA* promoter region was digested with *Nae*I, and inserted into the unique *Nae*I site of pCRA741, yielding pCRA742. Similarly, the *C. glutamicum ldhA* and *mdh* promoter regions were amplified by PCR using their respective oligonucleotide primers (primers 47–50) and *C. glutamicum* R chromosomal DNA as template. Each amplified PCR product was cloned into pCRA741, yielding pCRA743 for the *ldhA–lacZ* fusion and pCRA744 for the *mdh–lacZ* fusion (Table 1). The plasmids pCRA742, pCRA743 and pCRA744 were isolated as non-methylated DNA from *E. coli* JM110 for efficient gene introduction into *C. glutamicum* R (Vertès *et al.*, 1993a), and were subsequently integrated on the *C. glutamicum* R chromosome by markerless gene insertion methods, as described previously (Inui *et al.*, 2004a).

Primer extension. IRD700-labelled primers (primers 51–61) were designed as shown in Supplementary Table S1. Total RNA (100 μg) and 1.5 pmol primer were mixed and annealed at 80 °C for 90 min, at 60 °C for 90 min and at 30 °C for 90 min, using a GeneAmp PCR System 9700 instrument (Applied Biosystems). cDNA was synthesized at 42 °C for 1 h using AMV Reverse Transcriptase (Promega). The reaction was terminated by adding EDTA (pH 8.0) at a final concentration of 250 mM and DNase-free RNase A at a final concentration of 3 ng μl^{-1} to trigger degradation of the RNA templates. The resulting cDNA was treated by phenol/chloroform extraction and ethanol precipitation. Upon centrifugation, the precipitated DNA pellet was resuspended in IR2 Stop Solution (LI-COR). The primer extension products were treated at 95 °C for 2 min and placed on ice for 5 min, and separated on 3.7 % KB^{Plus} Gel Matrix (LI-COR) using a LI-COR 4300 DNA analyser. The migration position of each primer extension product was determined by comparing a sequencing ladder generated from a DNA fragment corresponding to the same chromosomal region, using the same primers and a DYEnamic Direct Cycle Sequencing kit with 7-deaza-dGTP (Amersham Biosciences).

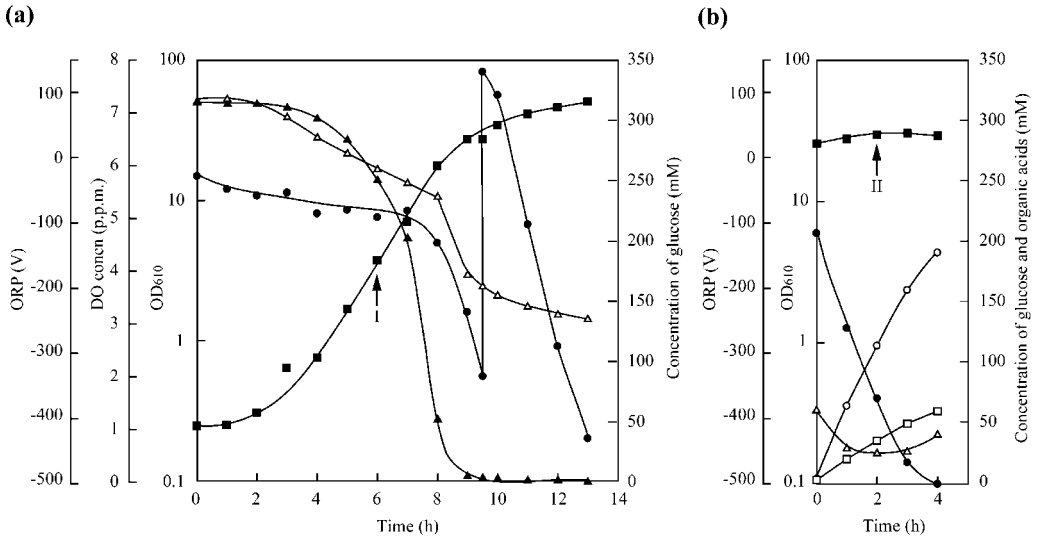

Fig. 1. Time-course of aerobic cultivation and oxygen deprived conditions, and sampling of *C. glutamicum* cells. Cell density (■), DO (▲) and ORP (△), and the concentration of glucose (●), lactate (○) and succinate (□) during aerobic cultivation (a) and oxygen deprived conditions (b) of *C. glutamicum* R. The arrows indicate the sampling points of *C. glutamicum* cells under aerobic (I) and oxygen deprivation conditions (II) for transcriptional analyses. Under oxygen deprivation conditions, the DO value was always maintained at a level lower than 0.01 p.p.m. A glucose spike was performed at 9.5 h after the beginning of the experiment by adding 20 g glucose to the reaction vessel containing 500 ml culture.

Gene disruption and replacement of the *mdh* and *sdhA* genes. Based on the *C. glutamicum* R whole genome sequence (Yukawa *et al.*, 2007), two oligonucleotide primers were designed to amplify a portion of the *mdh* gene (Supplementary Table S1). The oligonucleotide primers 62 and 63 were used in a PCR with *C. glutamicum* R chromosomal DNA as template. The 1.0 kb PCR product bearing the *mdh* gene was digested with *Bam*HI and *Sph*I, and inserted into the unique *Bam*HI–*Sph*I site of the *E. coli* vector pHSG398, which cannot replicate in *C. glutamicum,* yielding pCRA745. A 1.2 kb *Pst*I kanamycin cassette from pUC4K was blunt-ended with the Takara DNA blunting kit according to the manufacturer's instructions and subsequently inserted into the blunt-ended unique *Bgl*II site that lies within the *mdh* gene-coding region borne by plasmid pCRA745. The resulting plasmid pCRA746 was electroporated into *C. glutamicum* R according to the method that uses non-methylated DNA isolated from *E. coli*, as reported previously (Vertès *et al.*, 1993b). Similarly, the *C. glutamicum sdhA* gene was amplified by PCR using the oligonucleotide primers 64 and 65, and *C. glutamicum* R chromosomal DNA as template (Supplementary Table S1). The amplified PCR product was cloned into the *E. coli* vector pHSG398, yielding pCRA747. A 1.2 kb blunt-ended kanamycin cassette was inserted into the unique *Stu*I site of the *sdhA* gene on pCRA747. The resulting plasmid pCRA748 was electroporated into *C. glutamicum* R to generate an *sdhA*-deficient mutant. Disruptions of the two genes were confirmed by Southern hybridization and PCR analyses.

RESULTS

Transcriptome analysis of *C. glutamicum* during organic acid production under oxygen deprived conditions

Fig. 1 shows the time-course of the aerobic cultivation of *C. glutamicum* in a 1 l jar fermenter followed by its incubation under conditions of oxygen deprivation accompanied by the production of organic acid. We have previously reported that *C. glutamicum* cells produce organic acids from glucose at high yields in mineral medium, even though their proliferation is arrested (Inui *et al.*, 2004b; Okino *et al.*, 2005). Here, we confirmed that the glucose consumption rate during an oxygen deprived reaction [8.1 mmol (g DCW)$^{-1}$ h^{-1}] (Fig. 1b) was 1.4-fold higher than that attained during aerobic cultivation [6.0 mmol (g DCW)$^{-1}$ h^{-1}] (Fig. 1a). This phenomenon, which occurs in numerous organisms subjected to anaerobic conditions, is known as the 'Pasteur effect' (Emmerling *et al.*, 2000; Gottschalk, 1985).

In order to investigate the metabolic and molecular changes occurring at the transcriptional level when cells are shifted from aerobic cultivation to incubation under production-process conditions of oxygen deprivation without growth, we studied the global genetic expression pattern of *C. glutamicum* using DNA microarrays. Six independent DNA microarray experiments were performed to generate statistically significant data points that were satisfactory for gene expression analysis. Furthermore, profiling data for the genes coding for proteins involved in the glycolytic pathway, TCA cycle and H^+-ATPase were all verified by RT-PCR. Mid-exponential-phase cells were harvested after 6 h aerobic cultivation at a DO concentration of 5.7 p.p.m (ORP −17 mV) (Fig. 1a), and after 2 h incubation under oxygen deprivation conditions at a DO concentration of <0.01 p.p.m (ORP −451 mV) (Fig. 1b) for DNA microarray analysis.

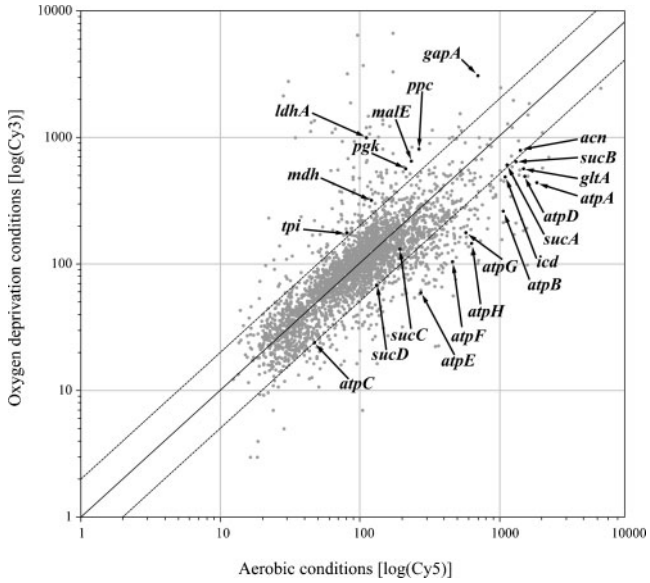

Fig. 2. Scatter plot of log(Cy3)- and log(Cy5)-derived fluorescence. Each dot represents the mean of six different experiments of duplicate spots of the same sample. The RNA of *C. glutamicum* R cells grown under aerobic conditions and without growth under oxygen deprivation conditions was used for Cy5 and Cy3 labelling. The two outer lines demarcate values for significant difference (two- and one-half-fold) in gene expression relative to the central line (no change in expression). The positions of several key enzyme-encoding genes (*gapA*, *pgk*, *tpi*, *ppc*, *ldhA*, *mdh*, *malE*, *gltA*, *acn*, *icd*, *sucA*, *sucB*, *sucC*, *sucD*, *atpB*, *atpE*, *atpF*, *atpH*, *atpA*, *atpG*, *atpD* and *atpC*) are indicated.

The ratios of mRNA levels in the cells under oxygen deprivation conditions relative to those attained under aerobic conditions were calculated by comparing normalized signal intensities between the two samples. The scatter plot of the resulting data showed a correlation coefficient of 0.37, demonstrating that significant changes in the gene expression profiles were taking place between the two conditions (Fig. 2). A total of 161 genes showed a greater than twofold increase in expression, and 221 genes were transcribed at levels less than half those observed under aerobic conditions (Supplementary Table S2). Using the nomenclature based on gene function as defined by the NCBI COG (Clusters of Orthologous Groups) database, 62 of the observed 161 upregulated genes and 64 of the observed 221 down-regulated genes belonged to the metabolism category, suggesting a profound change had occurred when cells were shifted from aerobic conditions to oxygen deprivation conditions (Supplementary Table S3). We focused our detailed analysis on the expression of genes coding for proteins involved in glycolysis, the anaplerotic pathway and the TCA cycle that are related to organic acid production under oxygen deprivation conditions. Several key enzyme-encoding genes in the glycolytic and anaplerotic pathways, and the reductive arm of the TCA cycle, were more than twofold upregulated (Table 2, Figs 2 and 3). In contrast, most genes in the oxidative arm of the TCA cycle (pyruvate→citrate→isocitrate→oxoglutarate→succinyl-CoA→succinate) were down-regulated (Table 2, Figs 2 and 3).

It has been demonstrated in previous work that in *C. glutamicum*, glycolysis under oxygen deprivation conditions is controlled at least in part by the intracellular NAD^+/NADH ratio. This conclusion is particularly based on the observation that the *gapA* gene, which encodes the enzyme GAPDH, is inhibited by NADH (Inui *et al.*, 2004a, b; Omumasaba *et al.*, 2004). Moreover, under oxygen deprivation conditions for succinate production by *C. glutamicum*, the major anaplerotic reaction is driven by the *ppc* gene product PEPC, rather than by the *pyc* gene product PC (Inui *et al.*, 2004b). The *gapA* and *ppc* genes form, with the *pgk* and *tpi* genes, a cluster in the *C. glutamicum* genome (Eikmanns, 1992). Consistent with these previous observations, we observed during the present study that these four genes were highly upregulated at the transcriptional level under oxygen deprivation conditions (Table 2, Figs 2 and 3). Furthermore, the *ldhA* gene, which codes for the enzyme LDH, was 8.6-fold induced at the transcriptional level under oxygen deprivation conditions (Table 2, Figs 2 and 3). Likewise, the *mdh* gene coding for MDH, an enzyme of the reductive arm of the TCA cycle, was 2.7-fold upregulated at the transcriptional level (Table 2, Figs 2 and 3). We have previously reported that *C. glutamicum fum* (fumarase; FUM) gene disruptants are unable to produce succinate (Inui *et al.*, 2004b). Similarly, we observed during the course of this work that two *C. glutamicum* mutants in which the MDH-encoding gene (*mdh*) or the succinate dehydrogenase (SDH) encoding gene (*sdhA*) had been disrupted were unable to produce succinate. These data indicate that MDH, FUM and SDH are all necessary for succinate production. Related to this finding, the *fum, sdhA, sdhB* and *sdhC* genes coding for enzymes of the reductive arm of the TCA cycle were all down-regulated under oxygen deprivation conditions (Table 2, Fig. 3). In addition, we have previously reported that overexpression in a *C. glutamicum ldhA* mutant of the *E. coli frdABCD* genes, encoding the enzyme fumarate reductase, which catalyses the conversion of fumarate to succinate, leads to a marginal albeit consistent increase in succinate production when cells are incubated under oxygen deprivation conditions (Murakami *et al.*, 2005). Thus, it was interesting that the *malE* gene, coding for the malic enzyme, was twofold overexpressed under oxygen deprivation conditions compared to aerobic conditions (Table 2, Figs 2 and 3). It was also noted that the *gltA, acn, icd, sucA, sucB, sucC* and *sucD* genes, which encode enzymes involved in the oxidative arm of the TCA cycle, were all down-regulated to approximately half to two-thirds of their expression levels under standard aeration conditions (Table 2, Figs 2 and 3). Moreover, the transcriptional expression of the *aceA* and *aceB* genes, respectively coding for isocitrate lyase and malate synthase, two enzymes of the glyoxylate shunt, were not significantly

Table 2. Expression data of *C. glutamicum* R genes in the glycolytic pathway, TCA cycle and H^+-ATPase

−, Not determined.

Gene	Enzyme	EC no.	DNA microarray	Quantitative RT-PCR*
Glycolysis				
ptsG	Phosphotransferase system, glucose-specific IIABC component	2.7.1.69	0.76	–
glk	Glucokinase	2.7.1.2	0.66	–
pgi	Glucose-6-phosphate isomerase	5.3.1.9	0.67	–
pfk	6-Phosphofructokinase	2.7.1.11	0.83	–
fba	Fructose-bisphosphate aldolase	4.1.2.13	0.97	–
tpi	TPI	5.3.1.1	2.23	2.59 (±0.21)
gapA	GAPDH A	1.2.1.12	4.20	3.85 (±0.30)
gapB	GAPDH B	1.2.1.12	0.44	–
acy	Acylphosphatase	3.6.1.7	0.80	–
pgk	PGK	2.7.2.3	2.81	2.76 (±0.13)
gpm	Phosphoglycerate mutase	5.4.2.1	1.12	–
eno	Enolase	4.2.1.11	1.09	–
pyk	Pyruvate kinase	2.7.1.40	0.83	–
ppsA	Phosphoenolpyruvate synthase	2.7.9.2	1.02	–
pdh	Pyruvate dehydrogenase	1.2.4.1	0.76	–
lpd	Dihydrolipoamide dehydrogenase	1.8.1.4	0.37	–
ldhA	L-LDH	1.1.1.27	8.59	6.68 (±0.62)
pyc	PC	6.4.1.1	1.05	–
ppc	PEPC	4.1.1.31	2.99	3.13 (±0.27)
pckA	Phosphoenolpyruvate carboxykinase	4.1.1.32	0.66	–
malE	Malic enzyme	1.1.1.40	2.34	2.32 (±0.21)
TCA cycle				
gltA	Citrate synthase	2.3.3.1	0.38	0.28 (±0.04)
acn	Aconitate hydratase	4.2.1.3	0.64	0.72 (±0.06)
icd	Isocitrate dehydrogenase	1.1.1.42	0.47	0.71 (±0.03)
sucA	2-Oxoglutarate dehydrogenase E1 component	1.2.4.2	0.66	0.71 (±0.04)
sucB	2-Oxoglutarate dehydrogenase E2 component	2.3.1.61	0.51	0.50 (±0.08)
sucC	Succinyl-CoA synthetase beta chain	6.2.1.5	0.63	0.63 (±0.05)
sucD	Succinyl-CoA synthetase alpha chain	6.2.1.5	0.51	0.50 (±0.04)
sdhA	SDH flavoprotein subunit	1.3.99.1	0.58	0.55 (±0.03)
sdhB	SDH iron–sulfur subunit	1.3.99.1	0.64	0.53 (±0.05)
sdhC	SDH cytochrome *b* subunit	1.3.99.1	0.54	0.58 (±0.03)
fum	FUM	4.2.1.2	0.89	0.91 (±0.04)
mdh	MDH	1.1.1.37	2.66	3.13 (±0.11)
mqo	MQO	1.1.99.16	0.70	0.46 (±0.05)
aceA	Isocitrate lyase	4.1.3.1	0.92	0.83 (±0.09)
aceB	Malate synthase	2.3.3.9	0.95	1.00 (±0.11)
H^+-ATPase				
atpB	H^+-ATPase a chain	3.6.3.14	0.29	0.34 (±0.05)
atpE	H^+-ATPase c chain	3.6.3.14	0.27	0.28 (±0.04)
atpF	H^+-ATPase b chain	3.6.3.14	0.28	0.26 (±0.04)
atpH	H^+-ATPase δ chain	3.6.3.14	0.29	0.28 (±0.03)
atpA	H^+-ATPase α chain	3.6.3.14	0.28	0.35 (±0.05)
atpG	H^+-ATPase γ chain	3.6.3.14	0.42	0.44 (±0.02)
atpD	H^+-ATPase β chain	3.6.3.14	0.40	0.29 (±0.04)
atpC	H^+-ATPase ε chain	3.6.3.14	0.59	0.18 (±0.06)

*The values are mean ± SD for three independent determinations.

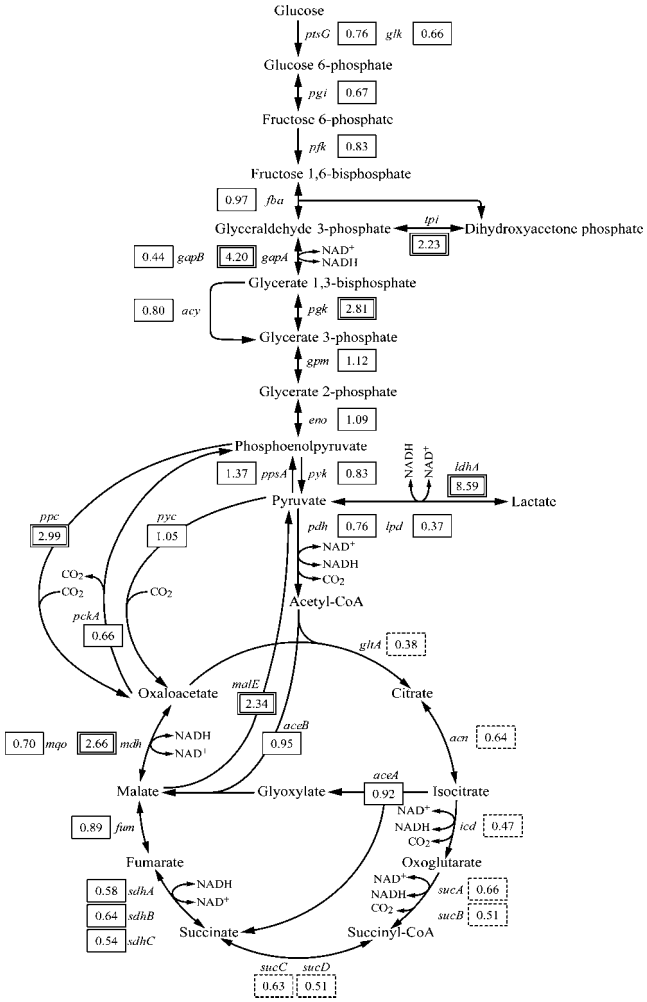

Fig. 3. Schematic representation of the glycolytic pathway and the TCA cycle exhibiting, relative to aerobic conditions, the mRNA levels of various genes in these pathways in cells incubated under oxygen deprivation conditions. The induction magnitudes for genes are reported in boxes. Double boxes indicate that the expression level was more than twofold increased; dotted boxes indicate down-regulated genes in the oxidative arm of the TCA cycle. The nomenclature of genes and their enzymes is shown in Table 2.

changed under oxygen deprivation compared to aerobic conditions (Table 2, Fig. 3). We have previously reported the absence of gas release by *C. glutamicum* during organic acid production under oxygen deprivation conditions (Inui *et al.*, 2004b) and that similar amounts of succinate are produced by *aceA* mutants compared to the wild-type (Inui *et al.*, 2004b). Together, these data corroborated the view that under oxygen deprivation conditions, *C. glutamicum* scarcely used either the forward direction of the TCA cycle, which is known to release CO_2 at several enzymic steps, or the glyoxylate shunt.

The DNA microarray data collected in this work were confirmed by quantitative RT-PCR analyses (Table 2).

Table 3. Enzymic activities of *C. glutamicum* R under aerobic and oxygen deprivation conditions

Enzyme	Specific activity* [nmol product min^{-1} $(mg\ protein)^{-1}$]	
	Aerobic conditions	Oxygen deprivation conditions
GAPDH	$4.9\ (\pm 0.1) \times 10^2$	$2.6\ (\pm 0.2) \times 10^3$
PGK	$2.0\ (\pm 0.2) \times 10^2$	$2.1\ (\pm 0.3) \times 10^3$
TPI	$2.3\ (\pm 0.3) \times 10$	$4.4\ (\pm 0.5) \times 10^2$
PEPC	$8.7\ (\pm 0.5) \times 10$	$3.9\ (\pm 0.3) \times 10^2$
LDH	$1.0\ (\pm 0.2) \times 10$	$1.4\ (\pm 0.2) \times 10^2$
MDH	$1.2\ (\pm 0.1) \times 10^2$	$3.1\ (\pm 0.2) \times 10^3$

*The values are mean ± SD for three independent determinations.

Furthermore, the increased gene expression at the transcriptional level was reflected in the corresponding specific enzyme activities when these were measured in parallel (Table 3). The ratios of the activities of the enzymes TPI and MDH when shifted from aerobic to oxygen deprivation conditions were notably higher than the ratios of their corresponding gene expression by the DNA microarray analysis (Tables 2 and 3). To understand the difference, additional analyses under oxygen deprivation conditions of mRNA stability, the efficiency and control of translation, and protease activity towards the enzymes, are needed.

DNA microarray and quantitative RT-PCR analyses furthermore revealed that transcription under oxygen deprivation conditions of the entire H^+-ATPase operon (including *atpB, atpE, atpF, atpH, atpA, atpG atpD* and *atpC*) is dramatically down-regulated to one-quarter to one-half of the levels attained under aerobic conditions (Table 2). These data suggest the existence of a correlation between reduced H^+-ATPase activity in *C. glutamicum* under oxygen deprivation conditions and enhanced glycolytic metabolism, as seen in H^+-ATPase mutants of *E. coli* (Jensen & Michelsen, 1992; Jensen *et al.*, 1995), *Bacillus subtilis* (Santana *et al.*, 1994) and *C. glutamicum* (Sekine *et al.*, 2001).

Effect of oxygen tension on expression of the *gapA* gene cluster, and the *ldhA* and *mdh* genes

The differences in transcriptional profiles between aerobic cultivation in A medium and the oxygen deprived reaction in BT medium could alternatively be explained by nutrient limitation, not simply oxygen tension. To verify whether the expression of the *gapA* gene cluster, and the *ldhA* and *mdh* genes, which were more than twofold upregulated in the above DNA microarray and quantitative RT-PCR analyses, were regulated via oxygen tension, we observed the changes of the expression of *gapA, pgk, tpi, ppc, ldhA* and *mdh* genes by supplying nitrogen gas during aerobic growth.

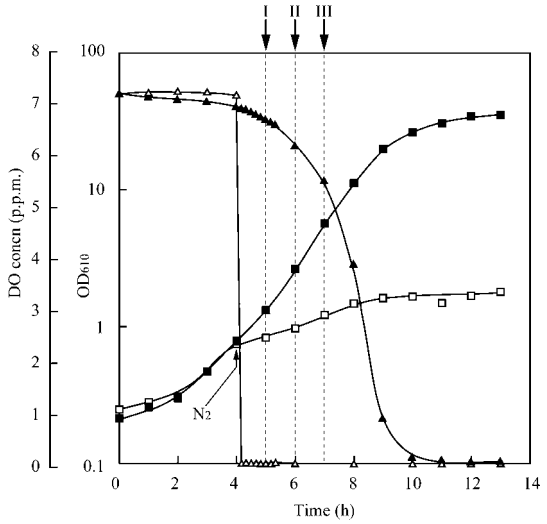

Fig. 4. Effect of supplying nitrogen gas during aerobic growth on the growth profile of *C. glutamicum* cells and the DO concentration. The cell density with air supply (■) and the concomitant DO (▲), and the cell density after supplying nitrogen gas from 4 h (□) and the concomitant DO (△), are shown. The arrows indicate the sampling points of *C. glutamicum* cells for transcriptional analysis. 'N_2' in the figure indicates the start point of nitrogen supply instead of air.

After 4 h aerobic growth (DO 6.9 p.p.m), a 99.9 % nitrogen gas supply was substituted for aeration (Fig. 4). DO was immediately reduced to 0.01 p.p.m. and the growth rate was drastically reduced. Cells after 5, 6 and 7 h (sampling points I, II and III in Fig. 4) of incubation were harvested from cultures supplied by air or nitrogen gas. Total RNAs were subsequently isolated from these samples and used for quantitative RT-PCR analysis.

The ratios of mRNA levels in the cells obtained by quantitative RT-PCR analysis under oxygen deprivation conditions after supplying nitrogen gas relative to those under aerobic conditions revealed that the *gapA, pgk, tpi, ppc, ldhA* and *mdh* genes were highly upregulated after 1, 2 and 3 h of nitrogen gas supply (after 5, 6 and 7 h of incubation) (Table 4). In particular, the *ldhA* gene was more highly upregulated than the others, and we observed that L-lactate production was immediately started after nitrogen was supplied (data not shown). These data confirmed that these genes were upregulated by decreased oxygen tension.

Time-course of gene expression under aerobic and oxygen deprivation conditions

To facilitate the study of the regulation of the expression of *gapA, ldhA* and *mdh*, three genes that are more than twofold upregulated under oxygen deprivation conditions, we integrated a monocopy of the *lacZ* fusion on the chromosome, in which *lacZ* expression was controlled by the transcriptional and translational regulatory signals of the *gapA, ldhA* and *mdh* genes. The effect of aerobic and oxygen deprivation conditions on *gapA, ldhA* and *mdh* expression was studied by measuring β-galactosidase levels in *C. glutamicum* that integrated each of these three *lacZ* fusions.

When *C. glutamicum* that integrated the *gapA–, ldhA–*, and *mdh–lacZ* fusions was grown in A medium under aerobic conditions, the expression of the three genes was strongly induced, and there was a reduction of the DO tension at the onset of the stationary phase (Fig. 5a, c, e). High-level expression of the *gapA–, ldhA–* and *mdh–lacZ* fusions was maintained under oxygen deprivation conditions (Fig. 5b, d, f).

Identification of the transcriptional start site

To localize the *gapA, ldhA* and *mdh* promoters, the transcriptional start sites of these three genes were determined by primer extension using as primers at least three 20-mer oligonucleotides having different 5′-end positions (Supplementary Table S1). Reverse-transcription experiments were performed using the same batches of total RNA as those used for DNA microarray analyses and extracted from *C. glutamicum* cells under aerobic condi-

Table 4. Effect of oxygen tension on expression of the *gapA* gene cluster, and the *ldhA* and *mdh* genes

Gene	Relative expression (nitrogen supply/aerobic) by quantitative RT-PCR*		
	After 5 h (sampling point I)†	After 6 h (sampling point II)†	After 7 h (sampling point III)†
gapA	6.09 (±0.41)	8.43 (±0.67)	3.62 (±0.19)
pgk	3.87 (±0.03)	6.18 (±0.18)	3.05 (±0.08)
tpi	4.03 (±0.32)	4.57 (±0.37)	2.62 (±0.17)
ppc	2.32 (±0.32)	2.75 (±0.30)	1.74 (±0.06)
ldhA	24.93 (±2.04)	24.46 (±2.13)	6.64 (±0.61)
mdh	9.41 (±0.71)	8.85 (±0.50)	3.61 (±0.44)

*The values are mean ± SD for three independent determinations.
†The sampling points in Fig. 4.

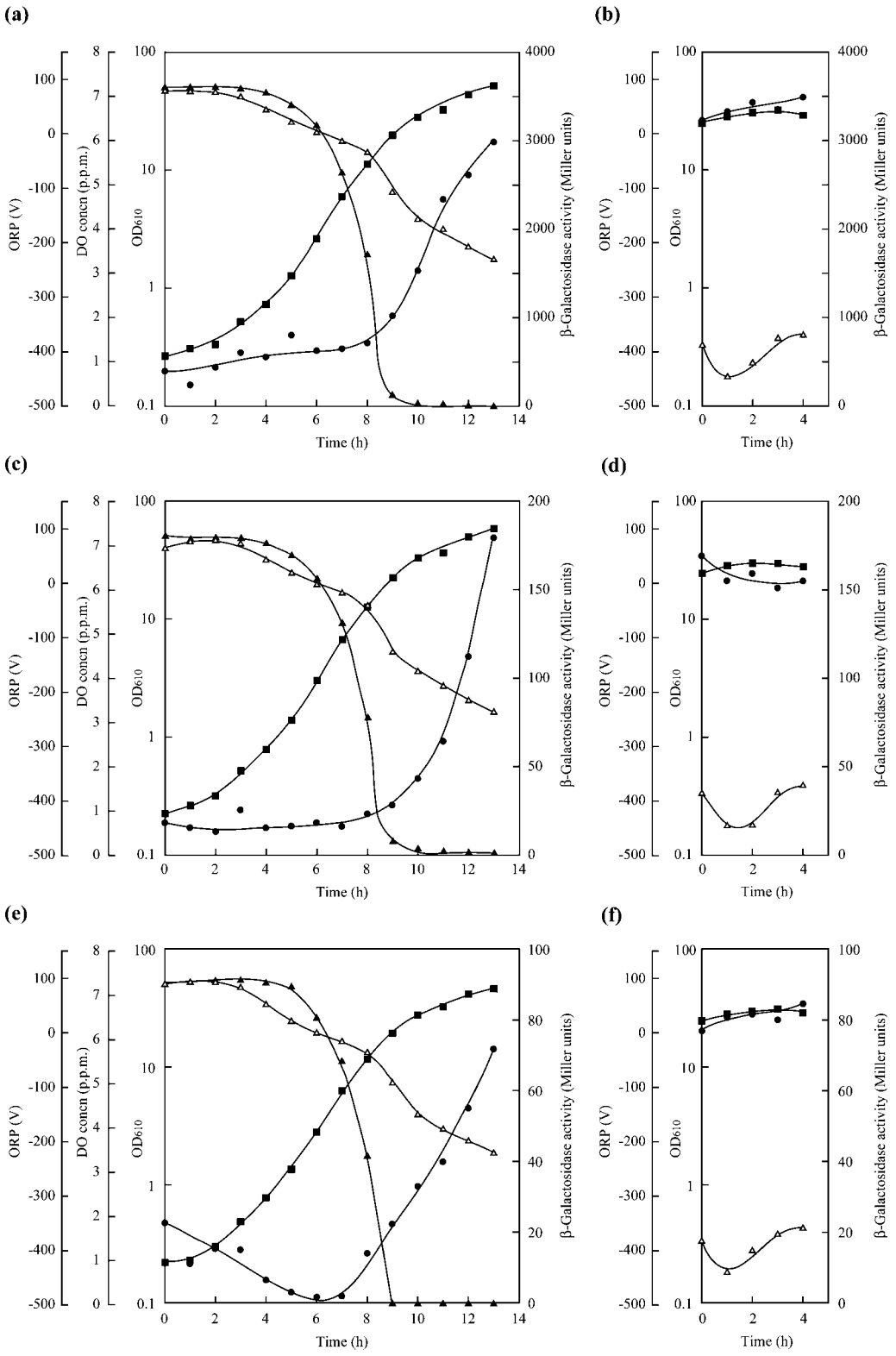

Fig. 5. Expression profiles of *gapA–*, *ldhA–* and *mdh–lacZ* fusion genes during aerobic cultivation and oxygen deprived conditions. Cell density (■), DO (▲), ORP (△) and *β*-galactosidase activity (●) are shown during aerobic cultivation (a, c, e) and oxygen deprived conditions (b, d, f) of *C. glutamicum* R integrating a *gapA–lacZ* fusion (a, b), a *ldhA–lacZ* fusion (c, d) and a *mdh–lacZ* fusion (e, f) on the chromosome.

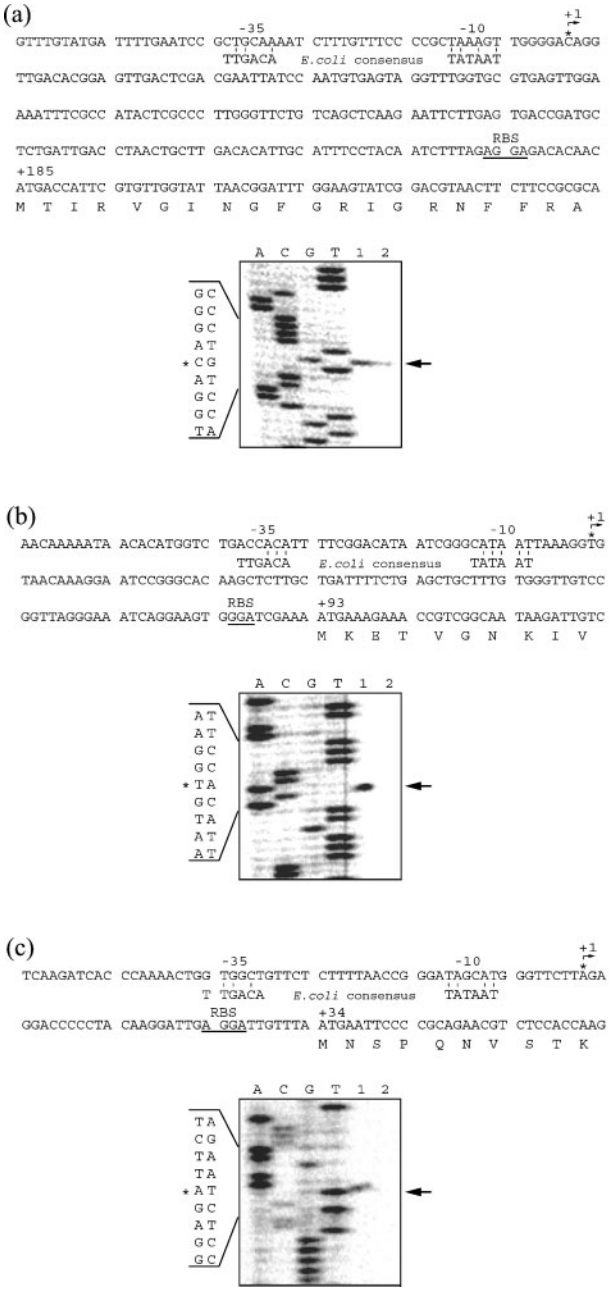

Fig. 6. Primer-extension analyses of the *gapA, ldhA* and *mdh* genes under oxygen deprivation and aerobic conditions. Sequence features upstream and downstream of the start point of transcription (upper figure) and sequencing gel analyses of primer extension (lower figure) are shown for the *gapA* (a), *ldhA* (b) and *mdh* (c) genes. For each sequence upstream of the start codon, a bent arrow marked +1 shows the start point of the transcript. Regions at distances canonical for promoters (−35 and −10 relative to the initiation codon) are indicated. The *E. coli* σ^{70} recognition consensus is represented underneath. Bases conserved between the two sequences are indicated by vertical bars. The putative ribosome binding site (RBS) is underlined. The first base of the start codon is indicated at position +185 for the *gapA* gene, +93 for the *ldhA* gene and +34 for the *mdh* gene, and the single-letter amino acid code for the amino terminus of the protein is presented below the sequence. For each sequencing gel analysed by primer extension, the products of high-resolution electrophoresis of 5′-labelled cDNA are shown aligned with a sequencing ladder generated from DNA from the same region, using the same primer. Dideoxy sequencing marker lanes A, C, T and G are indicated, and cDNA synthesis of the RNA samples is shown in lane 1 (under oxygen deprivation conditions) and lane 2 (under aerobic conditions). The migration position of the single primer extension product is indicated with an arrow. A portion of the DNA sequence is shown on the left, and the asterisk indicates the putative transcriptional start site.

tions (at point I in Fig. 1a) and oxygen deprivation conditions (at point II in Fig. 1b).

Primer-extension analyses of the *gapA, ldhA* and *mdh* genes revealed that, in all cases, a single major extension product was generated both under oxygen deprivation conditions (Fig. 6, lane 1) and aerobic conditions (Fig. 6, lane 2) with all three/four primers (Supplementary Table S1), corresponding to a 5′-end located 185, 93 or 34 bp upstream of the *gapA, ldhA* or *mdh* translation initiation codon, respectively. The results obtained with primer 51 for the *gapA* gene (Fig. 6a), primer 55 for the *ldhA* gene (Fig. 6b) and primer 58 for the *mdh* gene (Fig. 6c) are shown. The transcriptional signals of the *gapA, ldhA* and *mdh* genes under oxygen deprivation conditions were much stronger than those of the same genes under aerobic conditions, as observed in DNA microarray (Table 2, Fig. 3) and *lacZ* fusion (Fig. 5) experiments. Upstream of the transcriptional start sites of the *gapA, ldhA* and *mdh* genes, putative −10 and −35 promoter sequences, which share some similarities with the *E. coli* σ^{70} promoter consensus (Hawley & McClure, 1983), were observed. The transcriptional start site of the *gapA* gene in *C. glutamicum* R under oxygen deprivation conditions, as studied in this report, was identical to that in *C. glutamicum* ATCC 13032 grown under aerobic conditions and reported elsewhere (Schwinde *et al.*, 1993).

DISCUSSION

The adaptive response to oxygen deprivation conditions exhibited by *C. glutamicum* is similar to those previously observed in virtually every organism submitted to hypoxia. The genes coding for the main enzymes of the glycolytic pathway are upregulated at the transcriptional level, including *gapA*, *pgk*, *tpi* and *ppc*, which form a gene cluster in the *C. glutamicum* R genome (Yukawa *et al.*, 2007). However, the respective contributions of each of these enzymes to the increase of the glycolytic flux in *C. glutamicum* under oxygen deprivation conditions remain unclear.

Studies with a *gapA–lacZ* fusion suggest that the *gapA* gene is strongly induced at the onset of the stationary phase under aerobic growth conditions. Moreover, increased

expression of the *gapA* gene was sustained under oxygen deprivation conditions. The maintenance of the upregulation of *gapA* gene expression under oxygen deprivation conditions was consistently observed with three different methods: *lacZ* fusion, DNA microarray and quantitative RT-PCR.

Notwithstanding this observation, GAPDH activity has been demonstrated not to exert a significant control over the glycolytic flux in *Lactococcus lactis*, since the wild-type levels of this enzyme observed in this organism represent a three- to fourfold excess (Solem *et al.*, 2003). In addition, moderate overexpression of phosphofructokinase (*pfk*) and pyruvate kinase (*pyk*) has been shown not to dramatically modify flux ratios in *E. coli* (Sauer *et al.*, 1999). Perhaps the physiological significance of the latter observed transcriptional increases is limited, as recent studies in *E. coli* have demonstrated that, in this organism, the glycolytic flux is chiefly controlled by the intracellular demand for ATP, rather than by the overexpression of the enzymes of the pathway (Koebmann *et al.*, 2002a, b). On the other hand, PEPC, encoded by *ppc,* which belongs to the same gene cluster as *gapA*, is threefold upregulated in *C. glutamicum* R under oxygen deprivation conditions. Under these conditions, the OAA pool is replenished via conversion of phosphoenolpyruvate catalysed by PEPC, rather than via conversion of pyruvate through the action of the enzyme PC; this observation raises the question whether the pyruvate kinase step could be rate limiting (Inui *et al.*, 2004a, b), due either to redox imbalances or to insufficient pyruvate kinase activity. Pyruvate kinase has been shown elsewhere to be a controlling node of the corynebacterial glycolytic pathway, as it is subject to allosteric activation by AMP (Jetten *et al.*, 1994). Similarly, in *E. coli* under anaerobic conditions, the activity of the TCA cycle is reduced and anaplerosis via PEPC action predominantly generates OAA that feeds the reductive arm of the TCA cycle (Sauer *et al.*, 1999). PEPC overexpression enables succinate production by *C. glutamicum* under oxygen deprivation conditions, involving the subsequent exclusive action of MDH, as demonstrated by the inability of *C. glutamicum* MDH mutants to produce succinate. *C. glutamicum* possesses two types of L-malate dehydrogenase, MDH, a cytoplasmic, NAD-dependent malate dehydrogenase, and a highly active membrane-associated malate : quinone oxidoreductase (MQO) (Molenaar *et al.*, 1998). Under aerobic conditions, MQO, not MDH, is responsible for the net flux from malate to OAA within the TCA cycle (Eikmanns, 2005), and an MQO-deficient mutant is unable to grow on minimal medium, whereas an MDH-negative mutant has no obvious phenotype (Molenaar *et al.*, 2000). In addition, this enzyme may contribute to the backflux from OAA to fumarate, as detected by NMR flux quantification (Eikmanns, 2005). We therefore inferred that under oxygen deprivation, *mdh* gene expression is induced and MDH mainly functions for the backflux from OAA to fumarate with subsequent succinate production. The physiological value to the *C. glutamicum* cell under oxygen deprivation conditions of upregulating both *ppc* and *mdh*, which serve as key nodes in the metabolic network, is perhaps to commit the carbon chains to the reductive arm of the TCA cycle. A similar response is observed at the level of the expression of *ldhA*, which is present in a single copy in the *C. glutamicum* genome (Inui *et al.*, 2004b). The NAD-dependent LDH was 8.6-fold upregulated under oxygen deprivation conditions, perhaps to enable the cell to more efficiently regenerate its NAD^+ pool, and thus compensate, among other things, for the down-regulation of the oxidative arm of the TCA cycle and the cessation of energy-generating respiration.

Most genes in the oxidative arm of the TCA cycle, namely *gltA, acn*, *icd*, *sucA*, *sucB*, *sucC* and *sucD*, are down-regulated in *C. glutamicum* under oxygen deprivation conditions, which is consistent with the observation made in other organisms that under anaerobic conditions the primary function of the TCA cycle is to replenish biosynthetic precursors and not to generate energy. Likewise, the citrate synthase encoded by the *gltA* gene is down-regulated in oxygen-deprived C. *glutamicum*, similar to what is observed in *B. subtilis* (Nakano *et al.*, 1998). The physiological impact of this phenomenon remains to be elucidated.

The ubiquitous changes occasioned particularly by a sharp decrease in oxygen tension are apparent at the level of other energy components of the corynebacterial cell. For example, it is worth noting that transcription of the corynebacterial H^+-ATPase operon under oxygen deprivation conditions is sharply decreased to one-quarter to one-half of its level under aerobic conditions. This is in sharp contrast to what is observed in the facultative anaerobe *E. coli*, in which anaerobic cell growth on glucose minimal salts medium leads to H^+-ATPase expression that is 30 % higher than that attained under aerobic growth (Kasimoglu *et al.*, 1996). The physiological function of the ATPase complex is to generate ATP from ADP and P_i by electron transport-linked phosphorylation under aerobic conditions. Under non-respiratory conditions, the ATPase complex hydrolyses ATP to maintain an electrochemical gradient across the bacterial membrane. *E. coli* ATPase-deficient mutants exhibit increased flow through the TCA and glycolytic pathways (Jensen & Michelsen, 1992; Jensen *et al.*, 1995), with ATP being generated by an increased rate of glucose consumption and acetate generation. The increased flow through glycolysis and the TCA cycle results in an increased generation of NADH, which is compensated by an increased respiration rate without the generation of energy. Similarly, *B. subtilis* mutants grown aerobically consume twice the amount of glucose for the same increase in biomass, and exhibit increased synthesis of terminal oxidases, including ubiquinol oxidase and *a*-type haem, leading to an increased respiration rate, albeit also uncoupled from the generation of ATP (Santana *et al.*, 1994). H^+-ATPase mutant *C. glutamicum* also exhibits an increased respiration rate, an increased glucose consumption rate per cell, increased glycolysis, and decreased 2-

oxoglutarate production, suggesting a decreased flow through the oxidative arm of the TCA cycle, increased production and intracellular accumulation of pyruvate, and increased lactate production (Sekine *et al.*, 2001). Combined, these various observations suggest that, like *E. coli* and *B. subtilis*, *C. glutamicum* adjusts its metabolism in the absence of oxidative phosphorylation to maintain its energy level as high as possible, through mechanisms that, overall, have been highly conserved under different selective forces during two billion years of evolution since the divergence of Gram-negative and Gram-positive bacteria.

In *C. glutamicum*, and again similar to what is observed in *B. subtilis* (Ye *et al.*, 2000) and *E. coli* (Kang *et al.*, 2005), numerous other genes are induced or repressed with changes in environmental conditions such as oxygen tension. Among the genes observed to be highly inducible in the last two species, beyond those genes involved in anaerobic respiration, carbon metabolism and electron transport, iron uptake, stress response and several hypothetical genes are also upregulated. In *B. subtilis* and *E. coli*, the major regulator of the physiological switch between aerobic and anaerobic growth conditions is the DNA binding protein FNR (Gunsalus & Park, 1994; Kang *et al.*, 2005; Pao *et al.*, 1994; Ye *et al.*, 2000). For example, in *E. coli*, 297 genes constituting 184 different operons are regulated by FNR and/or oxygen levels (Kang *et al.*, 2005). However, other global transcriptional regulators have been shown to play important roles, such as ArcA, which impacts redox regulation, and whose knockout increases the activity of the TCA cycle by 60 % in *E. coli* (Perrenoud & Sauer, 2005). Similarly, down-regulation of the transcription of citrate synthase and aconitase in *B. subtilis* under anaerobiosis is driven by a mechanism that is different from those involving CcpA, CcpB, FNR and ResDE (Nakano *et al.*, 1998).

The overall physiological consequence of the observed increased transcription in corynebacteria under oxygen deprivation process conditions is an increased rate of carbon-source consumption, and presumably an increased flow of carbon through the glycolytic pathway and the reductive arm of the TCA cycle, accompanied by a concomitant increase in organic acid production. The numerous transcriptional changes observed under varying environmental conditions suggest the presence in *C. glutamicum*, as in other organisms, of one or more pleiotropic transcriptional regulators that are activated when cells are subjected to oxygen deprivation conditions and perhaps mediated by sensing-effector cascades. In addition to its fundamental scientific interest, the understanding of the molecular basis of the biological response of *C. glutamicum* to oxygen deprivation conditions will help design more efficient processes for industrial biotechnology.

ACKNOWLEDGEMENTS

We thank S. Murakami for technical support. We thank Roy H. Doi (University of California at Davis) and Crispinus A. Omumasaba (RITE) for critical reading of the manuscript. This work was financially supported in part by the New Energy and Industrial Technology Development Organization (NEDO), Japan.

REFERENCES

Billman-Jacobe, H., Wang, L., Kortt, A., Stewart, D. & Radford, A. (1995). Expression and secretion of heterologous proteases by *Corynebacterium glutamicum*. *Appl Environ Microbiol* **61**, 1610–1613.

Bunch, P. K., Mat-Jan, F., Lee, N. & Clark, D. P. (1997). The *ldhA* gene encoding the fermentative lactate dehydrogenase of *Escherichia coli*. *Microbiology* **143**, 187–195.

Eggeling, L. & Sahm, H. (1999). Amino acid production: principles of metabolic engineering. In *Metabolic Engineering*, pp. 153–176. Edited by S. Y. Lee & E. T. Papoutsakis. New York: Marcel Dekker.

Eikmanns, B. J. (1992). Identification, sequence analysis, and expression of a *Corynebacterium glutamicum* gene cluster encoding the three glycolytic enzymes glyceraldehyde-3-phosphate dehydrogenase, 3-phosphoglycerate kinase, and triosephosphate isomerase. *J Bacteriol* **174**, 6076–6086.

Eikmanns, B. (2005). Central metabolism: tricarboxylic acid cycle and anaplerotic reactions. In *Handbook of Corynebacterium glutamicum*, pp. 241–276. Edited by L. Eggeling & M. Bott. Boca Raton, FL: CRC Press.

Emmerling, M., Bailey, J. E. & Sauer, U. (2000). Altered regulation of pyruvate kinase or co-overexpression of phosphofructokinase increases glycolytic fluxes in resting *Escherichia coli*. *Biotechnol Bioeng* **67**, 623–627.

Gottschalk, G. (1985). *Bacterial Metabolism*, 2nd edn. New York: Springer.

Gunsalus, R. P. & Park, S. J. (1994). Aerobic-anaerobic gene regulation in *Escherichia coli*: control by the ArcAB and Fnr regulons. *Res Microbiol* **145**, 437–450.

Hawley, D. K. & McClure, W. R. (1983). Compilation and analysis of *Escherichia coli* promoter DNA sequences. *Nucleic Acids Res* **11**, 2237–2255.

Hermann, T. (2003). Industrial production of amino acids by coryneform bacteria. *J Biotechnol* **104**, 155–172.

Inui, M., Dumay, V., Zahn, K., Yamagata, H. & Yukawa, H. (1997). Structural and functional analysis of the phosphoenolpyruvate carboxylase gene from the purple nonsulfur bacterium *Rhodopseudomonas palustris* no. 7. *J Bacteriol* **179**, 4942–4945.

Inui, M., Terasawa, M. & Yukawa, H. (1999a). L-Isoleucine. In *Encyclopedia of Bioprocess Technology: Fermentation, Biocatalysis, and Bioseparation*, pp. 1498–1503. Edited by M. C. Flickinger & S. W. Drew. New York: Wiley.

Inui, M., Nakata, K., Roh, J. H., Zahn, K. & Yukawa, H. (1999b). Molecular and functional characterization of the *Rhodopseudomonas palustris* no. 7 phosphoenolpyruvate carboxykinase gene. *J Bacteriol* **181**, 2689–2696.

Inui, M., Kawaguchi, H., Murakami, S., Vertès, A. A. & Yukawa, H. (2004a). Metabolic engineering of *Corynebacterium glutamicum* for fuel ethanol production under oxygen deprivation conditions. *J Mol Microbiol Biotechnol* **8**, 243–254.

Inui, M., Murakami, S., Okino, S., Kawaguchi, H., Vertès, A. A. & Yukawa, H. (2004b). Metabolic analysis of *Corynebacterium glutamicum* during lactate and succinate productions under oxygen deprivation conditions. *J Mol Microbiol Biotechnol* **7**, 182–196.

Jensen, P. R. & Michelsen, O. (1992). Carbon and energy metabolism of *atp* mutants of *Escherichia coli*. *J Bacteriol* **174**, 7635–7641.

Jensen, P. R., Michelsen, O. & Westerhoff, H. V. (1995). Experimental determination of control by the H^+-ATPase in *Escherichia coli*. *J Bioenerg Biomembr* **27**, 543–554.

Jetten, M. S., Gubler, M. E., Lee, S. H. & Sinskey, A. J. (1994). Structural and functional analysis of pyruvate kinase from *Corynebacterium glutamicum*. *Appl Environ Microbiol* **60**, 2501–2507.

Kang, Y., Weber, K. D., Qiu, Y., Kiley, P. J. & Blattner, F. R. (2005). Genome-wide expression analysis indicates that FNR of *Escherichia coli* K-12 regulates a large number of genes of unknown function. *J Bacteriol* **187**, 1135–1160.

Kasimoglu, E., Park, S. J., Malek, J., Tseng, C. P. & Gunsalus, R. P. (1996). Transcriptional regulation of the proton-translocating ATPase (*atpIBEFHAGDC*) operon of *Escherichia coli*: control by cell growth rate. *J Bacteriol* **178**, 5563–5567.

Kelle, R., Hermann, T. & Bathe, B. (2005). L-Lysine production. In *Handbook of Corynebacterium glutamicum*, pp. 465–488. Edited by L. Eggeling & M. Bott. Boca Raton, FL: CRC Press.

Koebmann, B. J., Westerhoff, H. V., Snoep, J. L., Nilsson, D. & Jensen, P. R. (2002a). The glycolytic flux in *Escherichia coli* is controlled by the demand for ATP. *J Bacteriol* **184**, 3909–3916.

Koebmann, B. J., Westerhoff, H. V., Snoep, J. L., Solem, C., Pedersen, M. B., Nilsson, D., Michelsen, O. & Jensen, P. R. (2002b). The extent to which ATP demand controls the glycolytic flux depends strongly on the organism and conditions for growth. *Mol Biol Rep* **29**, 41–45.

Kumagai, H. (2000). Microbial production of amino acids in Japan. *Adv Biochem Eng Biotechnol* **69**, 71–85.

Molenaar, D., van der Rest, M. E. & Petrovic, S. (1998). Biochemical and genetic characterization of the membrane-associated malate dehydrogenase (acceptor) from *Corynebacterium glutamicum*. *Eur J Biochem* **254**, 395–403.

Molenaar, D., van der Rest, M. E., Drysch, A. & Yucel, R. (2000). Functions of the membrane-associated and cytoplasmic malate dehydrogenases in the citric acid cycle of *Corynebacterium glutamicum*. *J Bacteriol* **182**, 6884–6891.

Murakami, S., Nakata, K., Okino, S., Ikenaga, Y., Inui, M. & Yukawa, H. (2005). Coryneform bacterium transformant and process for producing dicarboxylic acid using the same. PCT patent application, WO 2005/010182 A1.

Nakano, M. M., Zuber, P. & Sonenshein, A. L. (1998). Anaerobic regulation of *Bacillus subtilis* Krebs cycle genes. *J Bacteriol* **180**, 3304–3311.

Okino, S., Inui, M. & Yukawa, H. (2005). Production of organic acids by *Corynebacterium glutamicum* under oxygen deprivation. *Appl Microbiol Biotechnol* **68**, 475–480.

Omumasaba, C. A., Okai, N., Inui, M. & Yukawa, H. (2004). *Corynebacterium glutamicum* glyceraldehyde-3-phosphate dehydrogenase isoforms with opposite, ATP-dependent regulation. *J Mol Microbiol Biotechnol* **8**, 91–103.

Pao, G. M., Tam, R., Lipschitz, L. S. & Saier, M. H., Jr (1994). Response regulators: structure, function and evolution. *Res Microbiol* **145**, 356–362.

Perrenoud, A. & Sauer, U. (2005). Impact of global transcriptional regulation by ArcA, ArcB, Cra, Crp, Cya, Fnr, and Mlc on glucose catabolism in *Escherichia coli*. *J Bacteriol* **187**, 3171–3179.

Peters-Wendisch, P. G., Schiel, B., Wendisch, V. F., Katsoulidis, E., Mockel, B., Sahm, H. & Eikmanns, B. J. (2001). Pyruvate carboxylase is a major bottleneck for glutamate and lysine production by *Corynebacterium glutamicum*. *J Mol Microbiol Biotechnol* **3**, 295–300.

Salim, K., Haedens, V., Content, J., Leblon, G. & Huygen, K. (1997). Heterologous expression of the *Mycobacterium tuberculosis* gene encoding antigen 85A in *Corynebacterium glutamicum*. *Appl Environ Microbiol* **63**, 4392–4400.

Sambrook, J., Fritsch, E. F. & Maniatis, T. (1989). *Molecular Cloning: a Laboratory Manual*, 2nd edn. Cold Spring Harbor, NY: Cold Spring Harbor Laboratory.

Santana, M., Ionescu, M. S., Vertès, A., Longin, R., Kunst, F., Danchin, A. & Glaser, P. (1994). *Bacillus subtilis* F_0F_1 ATPase: DNA sequence of the *atp* operon and characterization of *atp* mutants. *J Bacteriol* **176**, 6802–6811.

Sauer, U., Lasko, D. R., Fiaux, J., Hochuli, M., Glaser, R., Szyperski, T., Wuthrich, K. & Bailey, J. E. (1999). Metabolic flux ratio analysis of genetic and environmental modulations of *Escherichia coli* central carbon metabolism. *J Bacteriol* **181**, 6679–6688.

Schwinde, J. W., Thum-Schmitz, N., Eikmanns, B. J. & Sahm, H. (1993). Transcriptional analysis of the *gap-pgk-tpi-ppc* gene cluster of *Corynebacterium glutamicum*. *J Bacteriol* **175**, 3905–3908.

Sekine, H., Shimada, T., Hayashi, C., Ishiguro, A., Tomita, F. & Yokota, A. (2001). H^+-ATPase defect in *Corynebacterium glutamicum* abolishes glutamic acid production with enhancement of glucose consumption rate. *Appl Microbiol Biotechnol* **57**, 534–540.

Solem, C., Koebmann, B. J. & Jensen, P. R. (2003). Glyceraldehyde-3-phosphate dehydrogenase has no control over glycolytic flux in *Lactococcus lactis* MG1363. *J Bacteriol* **185**, 1564–1571.

Sridhar, J., Eiteman, M. A. & Wiegel, J. W. (2000). Elucidation of enzymes in fermentation pathways used by *Clostridium thermosuccinogenes* growing on inulin. *Appl Environ Microbiol* **66**, 246–251.

Suzuki, N., Okayama, S., Nonaka, H., Tsuge, Y., Inui, M. & Yukawa, H. (2005). Large-scale engineering of the *Corynebacterium glutamicum* genome. *Appl Environ Microbiol* **71**, 3369–3372.

Vertès, A. A., Inui, M., Kobayashi, M., Kurusu, Y. & Yukawa, H. (1993a). Presence of *mrr*- and *mcr*-like restriction systems in coryneform bacteria. *Res Microbiol* **144**, 181–185.

Vertès, A. A., Hatakeyama, K., Inui, M., Kobayashi, M., Kurusu, Y. & Yukawa, H. (1993b). Replacement recombination in coryneform bacteria: high efficiency integration requirement for non-methylated plasmid DNA. *Biosci Biotechnol Biochem* **57**, 2036–2038.

Vertès, A. A., Inui, M. & Yukawa, H. (2005). Manipulating corynebacteria, from individual genes to chromosomes. *Appl Environ Microbiol* **71**, 7633–7642.

Ye, R. W., Tao, W., Bedzyk, L., Young, T., Chen, M. & Li, L. (2000). Global gene expression profiles of *Bacillus subtilis* grown under anaerobic conditions. *J Bacteriol* **182**, 4458–4465.

Yukawa, H., Omumasaba, C. A., Nonaka, H., Kós, P., Okai, N., Suzuki, N., Suda, M., Tsuge, Y., Watanabe, J. & other authors (2007). Comparative analysis of the *Corynebacterium glutamicum* group and complete genome sequence of strain R. *Microbiology* **153**, 1042–1058.

Edited by: C. W. Chen